Journal of Thermal Analysis and Calorimetry, Vol. 92 (2008) 1, 161–167

EMANATION THERMAL ANALYSIS STUDY OF N-DOPED TITANIA PHOTOACTIVE POWDERS

V. Balek[1*], *J. Šubrt*[2], *I. M. Bountseva*[3], *H. Irie*[4] *and K. Hashimoto*[4,5]

[1]Nuclear Research Institute Řež, plc, 250 68 Řež, Czech Republic
[2]Institute of Inorganic Chemistry, ASCR, 250 68 Řež, Czech Republic
[3]Chemical Faculty, Moscow State University, 199234 Moscow, Russia
[4]Graduate School of Engineering, The University of Tokyo, 7-3-1 Hongo, Bunkyo-ku, Tokyo 113-8656, Japan
[5]Research Center for Advanced Science and Technology, The University of Tokyo, 4-6-1 Komaba, Meguro-ku, Tokyo 153-8904, Japan

Thermal behaviour of N-doped titania powders prepared by heat treatment of anatase in gaseous ammonia at 550 and 575°C, respectively, was characterized by emanation thermal analysis (ETA). The ETA results were used to assess transport properties of the samples subsurface using the mobility data of radon atoms previously incorporated into the samples to the depth of 60 nm. It was demonstrated that the radon permeability of anatase in the temperature range 50–500°C was enhanced for the N-doped titania as compared to the non-doped titania powder. Microstructure changes accompanying the anatase–rutile transition were pointed out from the decrease of the radon release rate in the temperature range 850–1000°C. The results of surface area and porosity measurements, DTA results as well XRD patterns supported the ETA results.

Keywords: *anatase, N-doped titania, DTA, ETA, porosity, surface area*

Introduction

Titania and doped titania have been recently applied in the environmental remediation, especially in water detoxification and air purification [1–3]. TiO_2 is an efficient photocatalyst, but UV light is necessary for its activation. Solar energy contains only about 4% UV light and much of the rest is visible light.

In order to utilize the visible (solar) light efficiently for the photo-catalytic reactions the titanium dioxide has to be modified. There have been several approaches how to modify the TiO_2. Several authors substituted Ti^{4+} in TiO_2 by metal ion implantation. Another approach is based on the formation of the Ti^{3+} sites by introducing the oxygen vacancies in TiO_2. It was reported [4] that it is possible to prepare the 'oxygen vacancy based – visible light sensitive titania' by the treatment of anatase under reductive hydrogen plasma.

N-doped titania photocatalyst sensitive to visible light irradiation was described in 2001 by Asahi *et al.* [5]. Since then, more than 3 hundreds papers were published on the preparation, characterization and application of the titania doped with nitrogen, for example, most recent papers published in 2006–2007 can be mentioned [6–24].

Irie *et al.* [25–27] prepared C-doped and N-doped titania powders. The $TiO_{2-x}N_x$ nanostructured powders were prepared [26] by the heat treatment of commercial anatase powder under the flow of gaseous ammonia at elevated temperatures of 550–600°C. In the samples prepared the amount of N introduced into $TiO_{2-x}N_x$ was depending on the temperature used for the titania heat treatment under the flow of gaseous ammonia, namely x values were lower than 0.02. The enhanced oxidation properties of the resulting $TiO_{2-x}N_x$ powder were evaluated by the decomposition of gaseous 2-propanol into CO_2, when irradiated under visible light in comparison with UV light [26].

In this paper emanation thermal analysis (ETA) [28] was used to characterize the thermal behavior of N-doped porous titania powder in comparison with a non-doped titania used as reference material. The ETA was already applied in our previous studies to characterize microstructure development on heating of titania powders as well as thin films [28–30].

Experimental

Samples

The N-doped titania powder samples were prepared by heating of the reference non-doped anatase powder under NH_3 gas flow at 550 and 575°C for 3 h, respectively.

A reference sample of non-doped titania powder was prepared by heat treatment of the initial anatase powder (ST-01, Ishihara Sangyo Kaisha Ltd., surface area 311 $m^2\ g^{-1}$) in air flow at 550°C for 3 h.

* Author for correspondence: bal@ujv.cz

1388–6150/$20.00

Akadémiai Kiadó, Budapest, Hungary
Springer, Dordrecht, The Netherlands

The chemical composition of the N-doped titania was $TiO_{2-x}N_x$, where x=0.005 and 0.011 for the samples prepared by etching of pure TiO_2 in NH_3 gas flow at 550 and 575°C for 3 h, respectively. The value of x was determined as the ratio of the XPS peak areas corresponding to 396 and 531 eV [26].

Methods

ETA and DTA measurements were carried out by using the ETA-DTA Netzsch equipment, Model 409 [28]. The radon labelled titania powder (sample amount of 0.05 g) was situated in a corundum crucible and heated in air in the temperature range 20–1050°C at the rate of 6°C min^{-1}. The constant air flow (flow rate 50 mL min^{-1}) took the radon released from the sample into the measuring chamber of radon radioactivity. Alumina powder was used as the DTA reference material.

The ETA results are presented as temperature dependencies of radon release rate E (in relative units); $E=A_\alpha/A_{total}$, where A_α is α-radioactivity of radon released in unit time from the labelled sample, and A_{total} is total γ-radioactivity of the labelled sample. The A_{total} value is proportional to the rate of radon formation in the sample. Semiconductor and NaI (Tl) detectors were used for the α- and γ-radioactivity measurements, respectively.

Scanning electron microscopy (SEM) equipment by Philips XL 30 CP was used for the characterization of surface morphology of the samples. Surface area and porosity of the samples were determined from nitrogen adsorption-desorption isotherms measured at liquid nitrogen temperature by a Coulter SA 3100 equipment by using the B.E.T. and B.J.H. methods, respectively. X-ray diffraction patterns were obtained by a Siemens D5005 equipment using CuK_α radiation (40 kV, 30 mA). Qualitative analysis was performed with the Eva Application and the Xpert HighScore using the JCPDS PDF-2 database.

X-ray photoelectron spectroscopy (XPS, PHI-5600, ULVAC-PHI Inc., Japan) with the monochromatic X-rays (MgK_α) was used to determine the N 1s spectra of the samples.

Results and discussion

From Table 1 it is obvious that etching of the pure titania powder in ammonia gas at 550 and 575°C for 3 h, respectively caused an increase of the surface area and porosity of the samples. For example, with the N-doped titania sample prepared at 575°C the surface area increased from 63 to 151 m^2 g^{-1} and the total porosity increased from 0.36 to 0.84 cm^3 g^{-1} in comparison with the pure non-doped titania.

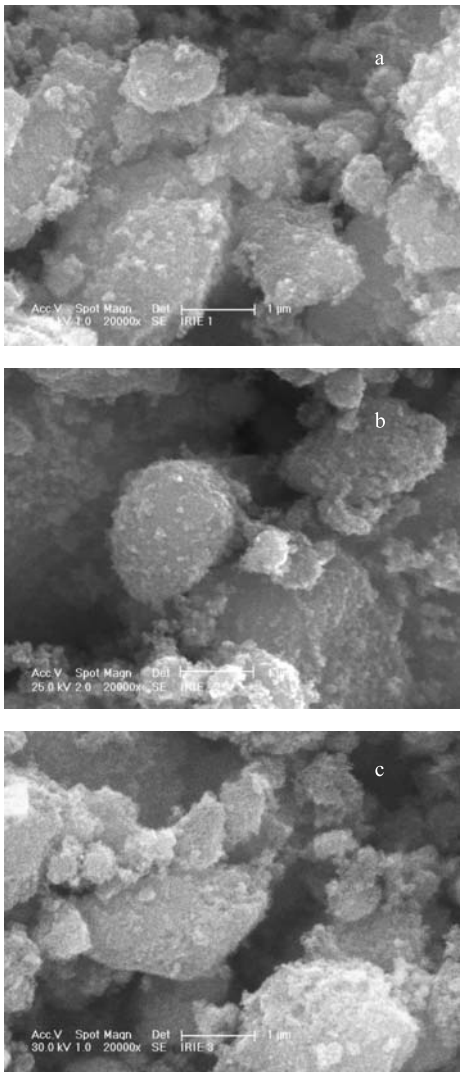

Fig. 1 SEM micrographs of a – the reference non-doped titania powder and of the N-doped titania powder prepared by etching of the non-doped titania for 3 h in a flow of NH_3 at b – 550°C and c – 575°C

Table 1 Characterization of the reference TiO_2 and $TiO_{2-x}N_x$ powders

Sample preparation	Reference non-doped anatase heated at 550°C/3 h in air	N-doped anatase prepared at 550°C/3 h in NH_3	N-doped anatase prepared at 575°C/3 h in NH_3
x value in $TiO_{2-x}N_x$	0	0.005	0.011
Surface area/m^2 g^{-1}	63.3	80.6	151.3
Total porosity/cm^3 g^{-1}	0.357	0.469	0.839

SEM micrographs in Fig. 1 showed no significant differences in surface morphology of the pure non-doped titania (a) and the N-doped titania prepared by etching of the pure titania in ammonia gas at 550°C/3 h (b) and of 575°C/3 h (c), respectively.

From XRD patterns in Fig. 2, curve 2 it followed that the N-doped sample prepared by etching of the pure titania powder in ammonia gas at 575°C/3 h was homogeneous anatase, as no peaks of TiN were observed. The XRD pattern of the pure anatase titania powder is presented for comparison in Fig. 2 as curve 1.

Figures 3a–c depict results of ETA and DTA of the pure titania powder and N-doped titania prepared by the etching of the pure titania with ammonia gas at temperatures of 550°C/3 h and 575°C/3 h, respectively.

The ETA data in Figs 3a–c were used to characterize the mobility of radon atoms and microstructure changes during heating of the samples in air. The ETA experimental data (points) were evaluated by using the theoretical approach proposed in [28, 31, 32]. Model curves obtained by fitting with the experimental ETA data are presented in Figs 3a–c as full lines.

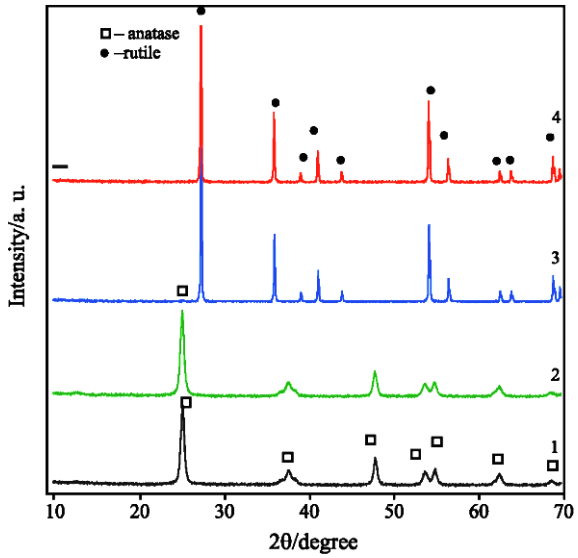

Fig. 2 XRD patterns of 1 – the reference non-doped titania and 2 – N-doped titania as prepared and N-doped titania heated to 3 – 800 and 4 – 950°C

DTA results (Figs 3a–c), measured simultaneously with ETA, were used to characterise the anatase-rutile transition of the titania samples as an exothermal effect. The exact temperatures of the DTA and ETA effects of the titania samples investigated in this study are summarized in Table 2.

From the DTA results in Fig. 3a it followed that the anatase-rutile transition of the pure titania was characterized by an exothermal effect with maximum at 865°C, whereas the maxima of the DTA exothermal effects corresponding to the A-R transition in the N-doped titania samples were observed at 922 and 935°C, respectively (Table 2). This is in agreement with the results of other authors [33–35] who found that anatase–rutile transition took place on heating to the temperatures 800–900°C.

As to the ETA results (Figs 3a–c) we assumed that the increase of the radon release rate, $E(T)$, observed in the temperature range 50–800°C was due to the radon diffusion along structure irregularities in anatase grains. The anatase-rutile transition and grain growth of the rutile grains was characterized by a decrease of the radon release rate in the temperature range of 800–950°C. We supposed that the decrease of the radon release rate, $E(T)$ observed in the temperature range of 800–950°C was due to healing of microstructure irregularities in the titania samples.

In order to support this suggestion about changes of the structure irregularities of the N-doped titania samples we shall use high resolution transmission electron spectroscopy (HRTEM) in our next study. In this study we have found that the surface area and total porosity values of the N-doped titania sample heated to 950°C decreased to 2.7 $m^2\ g^{-1}$ and 0.016 $cm^3\ g^{-1}$, respectively in comparison with the 'as prepared' sample.

SEM micrographs in Fig. 4 confirmed that a significant grain growth took place in the N-doped titania sample heated to 950°C (Fig. 4c). Nevertheless, a grain growth was observed also in the N-doped titania sample heated to 800°C (Fig. 4b) as compared to the 'as prepared' N-doped titania sample (Fig. 4a).

Moreover, from the XRD patterns in Fig. 2, curve 4, it followed that in N-doped titania sample

Table 2 Anatase-rutile transition of TiO_2 and $TiO_{2-x}N_x$ characterized by DTA and ETA

Sample preparation	ETA results		DTA exothermal effect
	Break of $E(T)$/°C	Maximum rate of $E(T)$ decrease/°C	T_{max}/°C
Reference sample: TiO_2 prepared from anatase ST 01 Ishihara Ltd. by heating at 550°C for 3 h in air	861	886	865
$TiO_{2-x}N_x$ prepared by heating TiO_2 sample in a flow of NH_3 at 550°C for 3 h	867	929	922
$TiO_{2-x}N_x$ prepared by heating TiO_2 sample in a flow of NH_3 at 575°C for 3 h	903	967	935

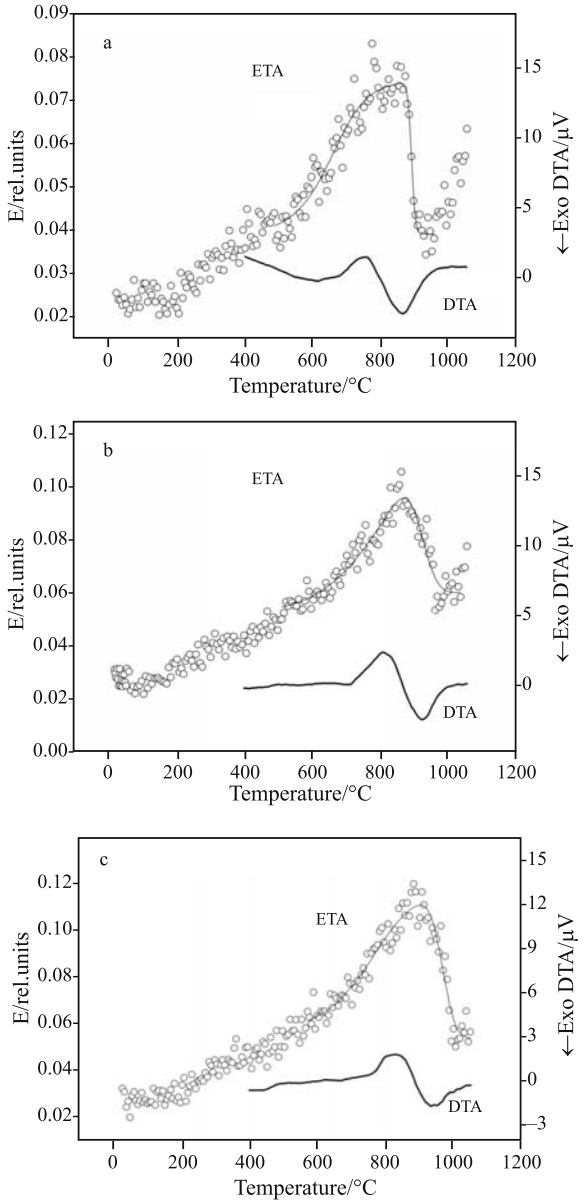

Fig. 3 ETA experimental results (round points) and model curves obtained by fitting with the experimental results (full lines) for the following samples. a – pure non-doped TiO_2 used as reference sample for the preparation of N-doped titania; b – N-doped titania prepared by heating the reference non-doped sample in a flow of NH_3 at 550°C/3 h; c – N-doped titania prepared by heating sample the reference non-doped titania in a flow of NH_3 at 575 °C/3 h

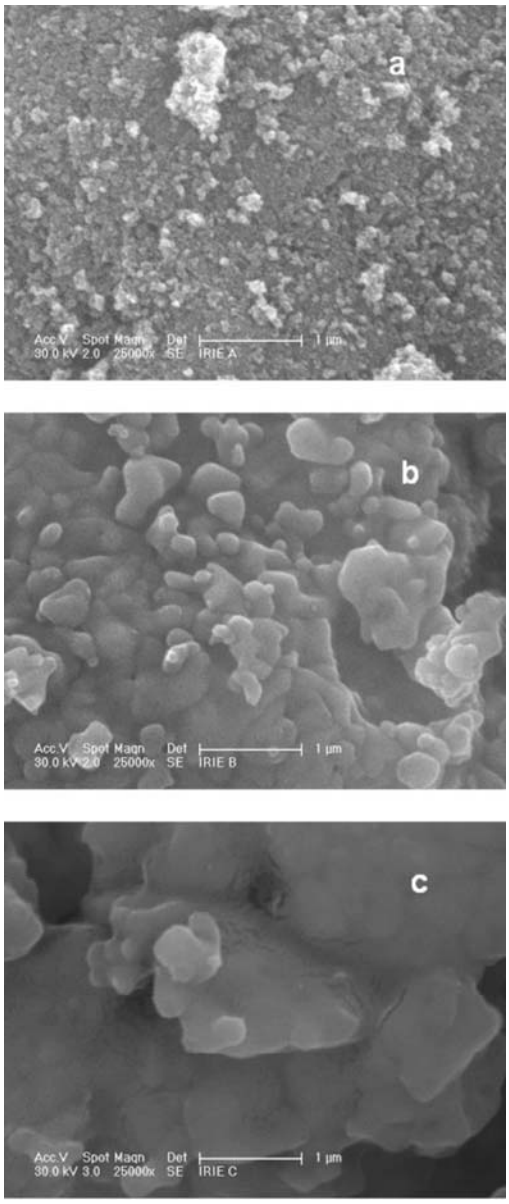

Fig. 4 SEM micrographs of N-doped titania samples annealed to temperature a – 500, b – 800 and c – 950°C. The N-doped titania powder was prepared by etching of the non-doped titania powder at a flow of NH_3 at 575°C/3 h

heated to 950°C the complete transition of anatase into rutile took place, whereas in the sample heated to 800°C (Fig. 2, curve 3) only small amount of anatase phase was found and mainly rutile phase was present.

Figure 5 depicts results of X-ray photoelectron spectroscopy (XPS) – N 1s spectra – of the N-doped titania samples and subsequently annealed to 800°C (curve 1) and to 950°C (curve 2), respectively. From the XPS results it followed that the N-doped titania annealed to 800°C was still of the chemical composition $TiO_{2-x}N_x$, but it was transformed into the non-doped TiO_2 after annealing to 950°C in air.

Evaluation of ETA results and transport properties of porous titania

From Figs 3a–c it followed that experimental ETA results and model curves of the temperature dependences of the radon release rate are in a good agreement. The ETA results characterized differences in

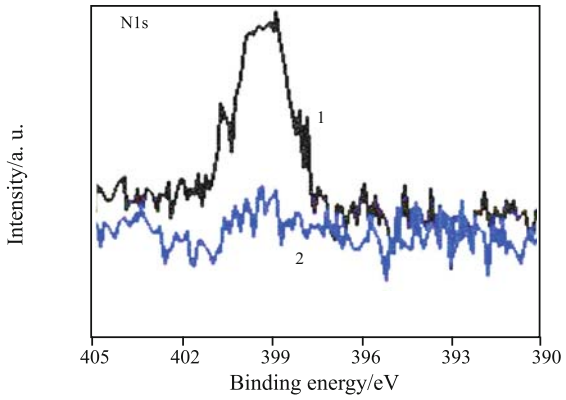

Fig. 5 XPS spectra of the N-doped titania prepared at a flow of NH_3 at 575°C/3 h and heated to 1 – 800 and 2 – 950°C

radon mobility and in the annealing of subsurface structure irregularities, serving as radon diffusion paths. The results of the radon diffusion parameters evaluated from the ETA data are summarized in Table 3.

The microstructure development on heating of the investigated titania samples was quantitatively described by a mathematical model [31, 32, 36]. The fitting of the model with ETA experimental data enabled us to evaluate transport properties of the N-doped titania in comparison with the properties of the reference non-doped titania powder.

It has been supposed that ^{220}Rn atoms were incorporated to the depth of 60 nm from the surface and were trapped in the subsurface of the sample; the structural irregularities served as paths for the radon atoms released by diffusion. We assumed that the increase of the radon release rate, $E(T)$, observed on heating in the temperature range 50–800°C (Figs 3a–c) was due to the radon diffusion along structure irregularities in the subsurface of grains. The random 'single jump' diffusion mechanism of radon was supposed to control the release of radon in this temperature range.

The radon release rate, $E(T)$, can be written [24] as

$$E(T)=E_{25}+E_D(T)\Psi(T) \quad (1)$$

where the term E_{25} is radon release rate measured at room temperature, the term E_D is radon release rate due to the diffusion, depending on the number of radon diffusion paths. The term E_D characterizes radon mobility along structure irregularities and $\Psi(T)$ is the function characterizing the decrease of the number of the radon diffusion paths.

The radon release rate, E_D, due to diffusion can expressed as

$$E_D=(3/y)(\coth y-\{1/y\}) \quad (2)$$

where

$$y(T)=(S/M)\rho/(D/\lambda)^{1/2}$$

where S/M is surface area and space of interfaces serving as radon diffusion paths, ρ is density of the sample, $(D/\lambda)^{1/2}$ is average radon diffusion length, D is radon diffusion coefficient and λ is radon decay constant ($\lambda=0.00127\ s^{-1}$).

$$D=D_0\exp(-Q/RT)$$

where D_0 is the factor depending on the number of diffusion paths and their availability for radon atoms migration, Q_D is activation energy of radon migration involving both the activation energy of the escape of radon atoms from the traps in the solid sample and that of the migration along diffusion paths in the solid, R=8.314 J mol^{-1} K^{-1} is molar gas constant, T is temperature in K.

Following expression for $\Psi(T)$ functions was proposed [35, 36] to describe the decrease of the number of radon diffusion path due to changes of the microstructure

$$\Psi(T)=0.5\left[1+\mathrm{erf}\frac{1-\frac{T_m}{T}}{\frac{\Delta T\sqrt{2}}{T}}\right] \quad (3)$$

where erf is the sign for the integral Gauss function, T_m is the temperature of maximum healing rate of the

Table 3 Characteristics of radon permeability of TiO_2 and $TiO_{2-x}N_x$ evaluated from ETA results

Sample notation and preparation	Radon permeability characteristics Temperature range 20–500°C	
	D_0/cm^2 s^{-1}	Q_D/kJ mol^{-1}
Reference sample: TiO_2 prepared from anatase ST-01 Ishihara Ltd. by heating at 550°C for 3 h in air	$8.4\cdot10^{-10}$	64±5
$TiO_{2-x}N_x$ prepared by heating TiO_2 sample in a flow of NH_3 at 550°C for 3 h	$7.8\cdot10^{-12}$	37±5
$TiO_{2-x}N_x$ prepared by heating TiO_2 sample in a flow of NH_3 at 575°C for 3 h	$1.8\cdot10^{-11}$	43±5

microstructure defects that serve as radon diffusion paths, ΔT is the temperature interval of the respective solid-state process.

The experimental ETA results were evaluated by means of the mathematical model. The temperature dependencies of radon release rate, E_D due to diffusion, were calculated by using Eq. (2). The temperature dependencies of $\Psi(T)$ functions, that characterized the healing of surface and subsurface structure irregularities, were calculated by using Eq. (3).

Figure 6 depicts temperature dependencies of ln$D$ *vs.* $1/T$ calculated from the ETA results measured on heating in the temperature range 50–500°C of the pure titania sample (curve 1) and of the two N-doped titania samples prepared in this study (curves 2 and 3), respectively. It is obvious that the relatively highest value of the activation energy Q_D of radon diffusion corresponds to the non-doped titania (Table 3).

It was assumed that the differences in transport properties of the titania samples investigated are due to the microstructure changes caused by the etching pure titania powder in gaseous ammonia during preparation of the N-doped titania samples.

Figure 7 depicts the model curves of the temperature dependences of the radon release rate $E(T)$ obtained by fitting with ETA experimental data in the range 500–1050°C. The functions $\Psi(T)$ were used to describe the healing of subsurface structure irregularities that served as radon diffusion paths in the samples during heating in air.

Figure 8 depicts temperature dependencies of the functions $\Psi(T)$ and the derivative functions $d\Psi(T)/dT$. As it follows from the $d\Psi(T)/dT$ dependencies, the maximum rate of the decrease of the number of radon diffusion paths due to healing of microstructure irregularities of non-doped titania was observed at 886°C, whereas the temperatures of 927 and 967°C indicated maximum rates of healing of micro-

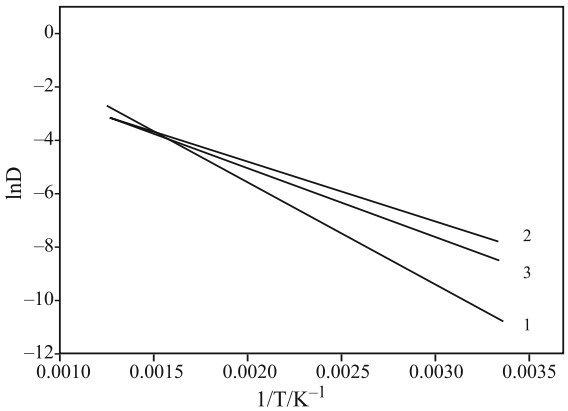

Fig. 6 Temperature dependencies of ln$D$ *vs.* $1/T$ for the 1 – non-doped titania sample and samples of N-doped titania prepared by heating in a flow of NH_3 at 2 – 550°C/3 h and at 3 – 575°C/3 h

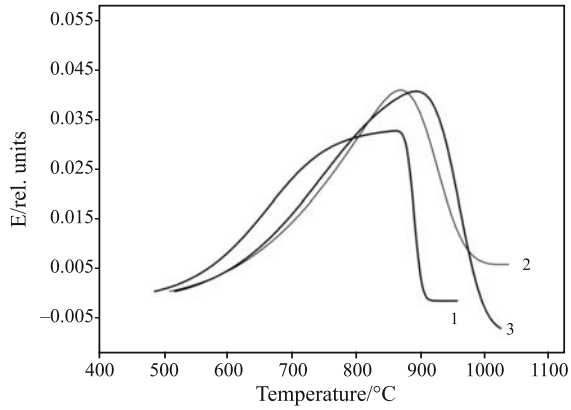

Fig. 7 Model curves of the temperature dependences of the radon release rate $E(T)$ for the 1 – non-doped titania sample and samples of N-doped titania prepared by heating of the non-doped titania samples in a flow of NH_3 at 2 – 550°C/3 h and at 3 – 575°C/3 h

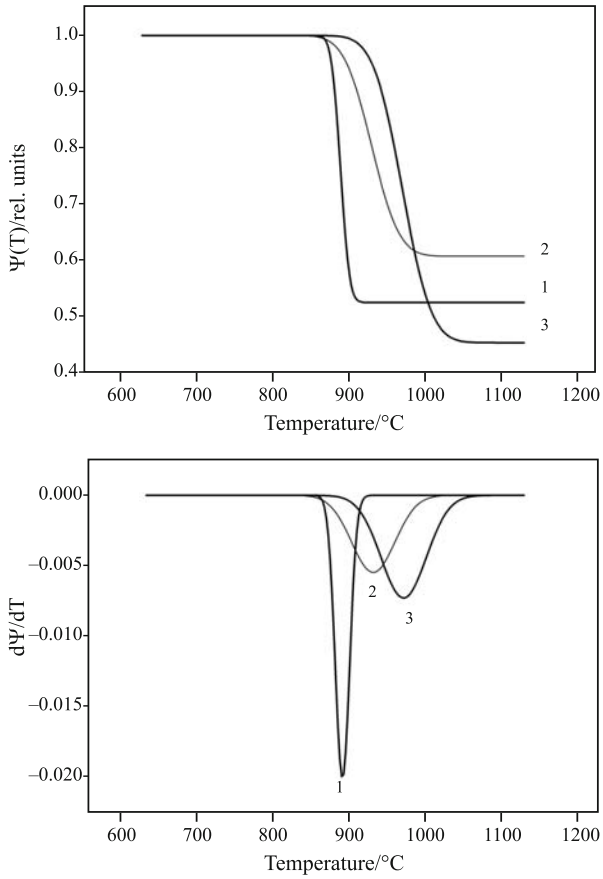

Fig. 8 Temperature dependencies of the functions $\Psi(T)$ and the derivative functions $d\Psi(T)/dT$ for the 1 – non-doped titania sample and samples of N-doped titania prepared in a flow of NH_3 at 2 – 550°C/3 h and at 3 – 575°C/3 h

structure irregularities for the N-doped titania samples prepared at 550 and 575°C, respectively (Table 2).

Conclusions

Transport properties of the N-doped titania powders prepared by heat treatment of anatase in gaseous ammonia at 550 and 575°C, respectively were characterized by using the results of ETA. It was demonstrated that the radon permeability of anatase observed by ETA in the temperature range 50–500°C was enhanced for the N-doped titania as compared to pure non-doped titania powder. Microstructure changes accompanying the anatase–rutile transition were characterized by ETA from the decrease of the radon release rate in the temperature range 850–1000°C. The results of surface area and porosity measurements, DTA results, XRD patterns and SEM micrographs supported the ETA data.

Acknowledgements

This work was supported in part by the Ministry of Education of the Czech Republic (Projects ME-879, LA-292 and 1M4531433201) and by the Ministry for Science, Education, Sports and Culture of Japan. Thanks are also due to Mrs. Mgr. Elena Klosová and Mr. Michael Hoffmann for ETA-DTA measurements and the treatment of experimental results.

References

1 A. Sobczynski and A. Dobosz, Pol. J. Environ. Stud., 10 (2001) 195.
2 J. Peral, X. Domenech and D. F. Ollis, J. Chem. Technol. Biotechnol., 70 (1997) 117.
3 M. Mrowetz, W. Balcerski, A. J. Colussi and M. R. Hoffman, J. Phys. Chem. B, 108 (2004) 17269.
4 K. Takeuchi, I. Nakamura, O. Matsumoto, S. Sugihara, M. Ando and T. Ihara, Chem. Lett., (2000) 1354.
5 R. Asahi, T. Morikawa, T. Ohwaki, K. Aoki and Y. Taga, Science, 293 (2001) 269.
6 N. Bao, J. Sun, F. Zhang, Z. H. Ma and F. Liu, Chin. J. Inorg. Chem., 23 (2007) 101.
7 H. Y. Chen, A. Nambu, W. Wen, J. Graciani, Z. Zhong, J. C. Hanson, E. Fujita and J. A. Rodriguez, J. Phys. Chem. C, 111 (2007) 1366.
8 D. Herman, J. Sicha and J. Musil, Vacuum, 81 (2006) 285.
9 D. G. Huang, S. J. Liao, J. M. Liu, Z. Dang and L. Petrik, J. Photochem. Photobiol. A-Chem., 184 (2006) 282.
10 L. H. Huang, Z. X. Sun and Y. L. Liu, J. Ceram. Soc. Jpn., 115 (2007) 28.
11 S. K. Joung, T. Amemiya, M. Murabayashi and K. Itoh, Appl. Catal. A-Gen., 312 (2006) 20.
12 I. C. Kang, Q. W. Zhang, J. Kano, S. Yin, T. Sato and F. Saito, J. Photochem. Photobiol. A-Chem., 189 (2007) 232.
13 S. Livraghi, M. C. Paganini, E. Giamello, A. Selloni, C. Di Valentin and G. Pacchioni, J. Am. Chem. Soc., 128 (2006) 15666.
14 T. Matsumoto, N. Iyi, Y. Kaneko, K. Kitamura, S. Ishihara, Y. Takasu and Y. Murakami, Catal. Today, 120 (2007) 226.
15 E. A. Mintz, O. K. Kainda, S. Mehrabi, D. Collart and L. Moeti, Abstr. Pap. Am. Chem. Soc., 231 (2006).
16 S. C. Pillai, P. Periyat, R. George, D. E. McCormack, M. K. Seery, H. Hayden, J. Colreavy, D. Corr and S. J. Hinder, J. Phys. Chem. C, 111 (2007) 1605.
17 N. Serpone, J. Phys. Chem. B, 110 (2006) 24287.
18 J. W. Wang, W. Zhu, Y. Q. Zhang and S. X. Liu, J. Phys. Chem. C, 111 (2007) 1010.
19 Y. Wang, C. X. Feng, Z. S. Jin, J. W. Zhang, H. J. Yang and S. L. Zhang, J. Mol. Catal. A-Chem., 260 (2006) 1.
20 Y. Q. Wang, X. J. Yu and D. Z. Sun, J. Hazard. Mater., 144 (2007) 328.
21 B. Wawrzyniak, A. W. Morawski and B. Tryba, Int. J. Photoenergy, (2006).
22 X. L. Yan, T. Ohno, K. Nishijima, R. Abe and B. Ohtani, Chem. Phys. Lett., 429 (2006) 606.
23 K. S. Yang, Y. Dai, B. B. Huang and S. H. Han, J. Phys. Chem. B, 110 (2006) 24011.
24 V. Balek, D. Li, J. Šubrt, E. Večerníková, S. Hishita, H. Mitsuhashi and H. Haneda, J. Phys. Chem. Solids, 68 (2007) 770.
25 H. Irie, S. Washizuka, Y. Watanabe, T. Kako and K. Hashimoto, J. Electrochem. Soc., 152 (2005) E351.
26 H. Irie, Y. Watanabe and K. Hashimoto, J. Phys. Chem. B, 107 (2003) 5483.
27 Y. Sakatani, H. Ando, K. Okusako, H. Koike, J. Nunoshige, T. Takata, J. N. Kondo, M. Hara and K. Domen, J. Mater. Res., 19 (2004) 2100.
28 V. Balek, J. Šubrt, T. Mitsuhashi, I. N. Beckman and K. Györyova, J. Therm. Anal. Cal., 67 (2002) 15.
29 V. Balek, T. Mitsuhashi, I. M. Bountseva, H. Haneda, Z. Malek and J. Šubrt, J. Sol-Gel Sci. Technol., 26 (2003) 185.
30 H. Hirashima, H. Imai, M. Y. Miah, I. M. Bountseva, I. N. Beckman and V. Balek, J. Non-Cryst. Solids, 350 (2004) 266.
31 I. N. Beckman and V. Balek, J. Therm. Anal. Cal., 67 (2002) 49.
32 V. Balek, M. Beneš, Z. Malek, G. Matuschek, A. Kettrup and S. Yariv, J. Therm. Anal. Cal., 83 (2006) 61.
33 S. Bakardjieva, J. Šubrt, V. Stengl, M. J. Dianez and M. J. Sayagues, Appl. Catal. B-Environ., 58 (2005) 193.
34 J. Krysa, M. Keppert, J. Jirkovsky, V. Stengl and J. Šubrt, Mater. Chem. Phys., 86 (2004) 333.
35 A. Dassler, A. Feltz, J. Jung, W. Ludwig and E. Kaisersberger, J .Thermal Anal., 33 (1988) 803.
36 V. Balek and I. N. Beckman, J. Therm. Anal. Cal., 82 (2005) 755.

DOI: 10.1007/s10973-007-8755-7